Biochimica et Biophysica Acta 1838 (2014) 1274–1280

Contents lists available at ScienceDirect

Biochimica et Biophysica Acta

journal homepage: www.elsevier.com/locate/bbamem

Modification of FP-HIV activity by peptide sequences of GB virus C: A biophysical approach

O. Domènech [a], A. Ortiz [a,b], M. Pujol [a,b], I. Haro [c], M. Muñoz [a,b], M.A. Alsina [a,b], J. Prat [a,b], M.A. Busquets [a,b], V. Girona [a,b,*]

[a] Physical Chemistry Department, Faculty of Pharmacy, University of Barcelona, Institute of Nanoscience and Nanotechnology (IN2UB), Avda Joan XXIII, s/n. 08028 Barcelona, Catalonia, Spain
[b] Associated Unit to the CSIC Peptides and proteins: Physicochemical properties, Spain
[c] Unit of Synthesis and Biomedical Applications of Peptides, Department of Biomedical Chemistry (IQAB-CSIC), Jordi Girona 18–26, 08034 Barcelona, Spain

ARTICLE INFO

Article history:
Received 26 September 2013
Received in revised form 29 January 2014
Accepted 3 February 2014
Available online 11 February 2014

Keywords:
Synthetic peptides
Atomic force microscopy
FP-HIV
Fluorescence anisotropy

ABSTRACT

Three synthetic peptide sequences of 18 amino acid each, corresponding to different fragments of the E2 capsid protein of GB virus C (GBV-C): SDRDTVVELSEWGVPCAT (P45), GSVRFPFHRCGAGPKLTK (P58) and RFPFHRCGAGPKLTKDLE (P59) have been characterized in order to find a relationship between their physicochemical properties and the results obtained in cellular models. Experiments were performed in presence and absence of the HIV fusion peptide (FP-HIV) due to the evidences that GBV-C inhibits AIDS progression. P45 peptide showed lower surface activity and less extent of penetration into 1,2-dimyristoyl-*sn*-glycero-3-phosphocholine (DMPC) and 1,2-dimyristoyl-*sn*-glycero-3-phospho-L-serine (DMPS) (3:2, mol/mol) lipid monolayers than P58 and P59. However, P45 peptide presented higher capacity to inhibit FP-HIV induced cell–cell fusion than the other two sequences. These results were supported by fluorescence anisotropy measurements which indicated that P45 had a significant effect on the inhibition of FP-HIV perturbation of liposomes of the same lipid composition. Finally, atomic force microscopy (AFM) studies have evidenced the modification of the changes induced by the FP-HIV in the morphology of lipid bilayers when P45 was present in the medium.

1. Introduction

There are uncountable studies in the literature dealing with the use of synthetic peptides as simple tools for unraveling the properties of proteins involved in a great variety of processes or even substituting the whole protein for a specific function [1]. Peptides have been designed and synthesized for therapeutic applications. For instance as a treatment for autoimmune and rheumatic diseases [2,3], several modes of cancer [4–7] or as inhibitors of HIV-1 reverse transcriptase and integrase [8]. Due to the advantageous properties of synthetic peptides compared to biological molecules there is an increasing interest in replacing biological antigens by synthetic peptides as well as the use of site-specific antibodies induced with synthetic peptides in vaccine design [9–12]. Diagnosis has been another extensive application of synthetic peptides with successful results in autoimmune [13], HIV [14] and several forms of hepatitis infections [15,16], amyloid related diseases [17] or rheumatoid arthritis [3,18]. The interest of the synthetic peptides is supported by the increasing number of patents published.

From more than two decades, our group has been working with peptide sequences corresponding to fragments of structural and non-structural capsid proteins of hepatitis variants [15,18,19]. More recently, the evidence that the coexistence of GB virus C (GBV-C) and HIV is related to a decrease in AIDS progression has focused our efforts in the selection, synthesis and physicochemical characterization of GBV-C sequences and the analysis of their interaction with the HIV fusion peptide (FP-HIV). The studies were mainly based on the analysis of GBV-C peptides, FP-HIV, and their combination at different molar ratios in solution as well as their behavior in presence of lipid monolayers and liposomes as model membranes [20,21].

Despite the data obtained up to now studying the interaction of peptide sequences with mono and bilayers our main concern is to find a good correlation between the results obtained *in vitro* with those *in vivo*. In addition, we would like to figure out what is the role of GBV-C peptides in the decrease of HIV infectivity. To get insight into this aspect, we have chosen three peptide sequences SDRDTVVELSEWGVPCAT (P45), GSVRFPFHRCGAGPKLTK (P58) and RFPFHRCGAGPKLTKDLE (P59) corresponding to the E2 capsid protein of GBV-C that have shown different activity in several experiments. Thus, P45 and P59 showed inhibitory effect on the FP-HIV induced leakage assay but only P45 was capable to inhibit FP-HIV induce cell-cell fusion [22]. In the present paper, we compare the surface properties of these peptides alone or in presence of FP-HIV with the Langmuir technique [23] by analyzing both the ability of the peptides to change the surface activity of a buffered saline solution and, their incorporation into lipid monolayers of 1,2-dimyristoyl-*sn*-glycero-3-phosphocholine (DMPC) and 1,2-dimyristoyl-*sn*-glycero-3-

* Corresponding author. Tel.: +34 934 024 556; fax: +34 934 035 987.
E-mail address: vgirona@ub.edu (V. Girona).

http://dx.doi.org/10.1016/j.bbamem.2014.02.001
0005-2736

phospho-L-serine (DMPS) (3:2, mol/mol). This lipid composition was chosen for being a good model that mimics the lipid composition of the membranes infected by HIV [24,25]. Fluorescence anisotropy measurements with large unilamellar liposomes (LUVs) of the same lipid composition were used to measure the penetration depth of the peptides into the bilayer. Finally, atomic force microscopy (AFM) [26] was chosen to determine the morphological changes in the surface of DMPC/DMPS (3:2, mol/mol) supported lipid bilayers (SLB) driven by P45 in presence and absence of FP-HIV. Results conclude that P45 is likely the best candidate to inhibit FP-HIV.

2. Materials and methods

The phospholipids used in this study were 1,2-dimyristoyl-*sn*-glycero-3-phosphocholine (DMPC) and 1,2-dimyristoyl-*sn*-glycero-3-phospho-L-serine (sodium salt) (DMPS) from Avanti Polar Lipids (Alabaster, Al.). The lipids were pure as determined by thin layer chromatography and used as received. A mixture of chloroform and methanol (2:1, v/v) (HPLC grade Merck, Germany) was used to dissolve and as spreading solvent for all lipids. Water used was doubly distilled and deionized (Milli-Q system, Millipore Corp. 18.3 MΩ cm, resistivity).

Peptides in the amidated form were obtained by solid-phase peptide synthesis as previously described [22]. Stock peptide solutions of 1 mM were prepared in 20% acetonitrile (HPLC grade, Merck) in water.

The fluorescent probes 1-(4-trimethylammoniumphenyl)-6-phenyl-1,3,5-hexatriene p-toluenesulfonate (TMA-DPH) and 1,6-diphenyl-1,3,5-hexatriene (DPH) were purchased from Molecular Probes, Inc. (Invitrogen, Cralsbad, CA).

2.1. Surface activity measurements

The surface properties of the peptides were analyzed as described elsewhere [19] in a NIMA (Conventry, UK) film balance equipped with a Wilhelmy platinum plate and a round Teflon® dish (surface area 19.6 cm^2, 27.2 cm^3 of capacity) with Tris 10 mM, pH 7.4 as the subphase. The Teflon® trough and the plate were thoroughly cleaned before each run with chloroform and boiling water to avoid carry-over of lipid. Increasing volumes of a concentrated solution of the peptide were injected beneath the surface through a lateral whole. During the experiments, the subphase was continuously stirred. Surface pressure (π) with time was recorded until a steady-state value was obtained.

2.2. Peptide insertion into lipid monolayers

The kinetics of peptide binding to the lipid monolayers were monitored with the same Teflon® trough described above. Lipid monolayers at the required initial surface pressure, π_o, (5, 10, 20 or 32 mN m^{-1}) were formed by spreading the lipid from chloroform/methanol (2:1, v/v) solutions onto Tris 10 mM, pH 7.4 subphases. After 20 min for solvent evaporation and to assure monolayer stability, the peptide was injected from a stock solution in H_2O/ACN (1:1, v/v) beneath the lipid monolayer. The subphase was stirred continuously to ensure a homogeneous distribution and a good interaction of the peptide with the monolayer. Pressure increases ($\Delta\pi$) with time were recorded until no further changes occurred indicating that equilibrium was reached. For each sample, the values of $\Delta\pi$ as a function of various π_o values were obtained. The plot of $\Delta\pi$ versus π_o yields a straight line with negative slope which intersects the abscissa at a limiting surface pressure that is defined as the critical insertion pressure of the peptide for the corresponding lipid monolayer [27].

2.3. Compression isotherms

The compression isotherms were performed on a Langmuir film balance, NIMA equipped with a Wilhelmy platinum plate and a Teflon® trough of 595 cm^2 of surface area and a volume of 300 cm^3. The output of the pressure pickup was calibrated by recording the well-known isotherm of stearic acid that is characterized by a sharp phase transition at 25 mN m^{-1} for a subphase of pure water at 20°C. Peptide solutions were prepared by solving the appropriate amount in chloroform. Monolayers were formed by applying small drops of the spreading solutions on the Tris subphase with a microsyringe (Hamilton Co., Reno, NV). After 20 min for solvent evaporation, the monolayers of the desired composition were continuously compressed (symmetrical compression) with an area reduction rate of 10 nm^2 min^{-1} until the system had reached its compression limit. The temperature of the subphase was 21 ± 0.5°C. All samples were run at least three times in the direction of increasing pressure with freshly prepared films. In addition and to assess the stability of the monolayers, the film was submitted to compression and decompression cycles.

2.4. Liposome preparation

DMPC/DMPS (3:2, mol/mol) lipid vesicles were prepared as follows: lipid mixture was dissolved in chloroform/methanol (2:1, v/v) and the solution was dried by rotatory evaporation. The last traces of solvents were removed by keeping the sample under vacuum for at least 24 h. Tris buffer (10 mM, pH 7.4) was added to the lipids mixture to give a final concentration of 3.5 mM. Multilamellar vesicles (MLVs) were then prepared by vortexing the lipids suspension during 10 min. Large unilamellar vesicles (LUVs) were prepared by ten freeze–thaw cycles of MLVs followed by the extrusion of the preparations ten times through 100 nm pore-size polycarbonate filters (Nucleopore, Pleasanton, CA, USA) in a high pressure extruder (Lipex, Biomembranes, Vancouver, Canada). All over the experiments, the temperature was 45°C, which is above the transition temperature (T_m) of the lipid with higher T_m.

The size distribution of the vesicles was measured by dynamic light scattering with a Zetasizer Nano instrument (Malvern, EU) at 25°C. The particle size distribution was designated by the polydispersity index, which ranged from 0.0 for an entirely monodisperse sample, to 1.0 for a polydisperse sample. The z-average mean diameter was ~120 nm and polydispersity around 0.15. The phospholipid concentration of the preparations was determined by phosphorus quantification [28].

2.5. Fluorescence anisotropy of membrane lipids

Steady-state anisotropy measurements were carried with an Aminco Bowman AB2 (Microbeam, SA) spectrofluorimeter using L-format fluorescence polarizers. The dynamics of LUVs of DMPC/DMPS (3:2, mol/mol) in presence of E2 peptides was determined by measuring the degree of depolarization of fluorescence emitted from the probes DPH or TMA-DPH [29].

The excitation and emission wavelength were 365 and 425 nm, respectively for both probes (slit-widths: 4 nm). Labeled vesicles with 1% of the desired probe were mixed with the peptide in a 10 mM Tris at pH 7.4, and anisotropy was measured automatically. For each sample, two cycles were done: a heating cycle from 15°C up to 40°C, followed by a cooling cycle to the initial temperature, at 1°C intervals, allowing 5 min for thermal equilibration. All solutions were stirred continuously during the measurements. The temperature was controlled with a peltier system piloted by a computer program (Microbeam S.A., Barcelona, Spain), and registered with a thermocouple inserted into the cuvette. Fluorescence anisotropy I was calculated automatically by the software provided with the instrument, according to Eq. (1):

$$r = \frac{I_{Vv} - GI_{Vh}}{I_{Vv} + 2GI_{Vh}} \quad (1)$$

where I_{Vv} and I_{Vh} are fluorescence intensities of the emitted polarized light with the emission polarizer parallel or perpendicular, respectively,

Table 1
Peptide sequences and their physical chemistry properties. π_{sat}: saturation pressure; *K:* concentration needed to reach half of the maximum pressure; *Γ:* surface excess concentration and Area occupied per molecule.

Peptide	Amino acid sequence	Net charge pH 7.40	Isoelectric point	π_{sat} mN m^{-1}	*K* nM	Γ_{max} mol m^{-2}	*Area* nm^2 molec^{-1}
P 59	RFPFHRCGAGPKLTKDLE	**+3**	10.58	13.8	166.9	1.29×10^{-6}	1.29
P 58	GSVRFPFHRCGAGPKLTK	**+5**	12.42	21.9	219.4	1.84×10^{-6}	0.90
P 45	SDRDTVVELSEWGVPCAT	**−2**	4.05	8.0	378.9	0.77×10^{-6}	2.15
FP-HIV	AVGIGALFLGFLGAAGSTMGAAS	**+1**	14.0	79.5	521	4.75×10^{-6}	0.35

to the excitation polarizer. Anisotropy values were corrected for dependencies in the detection system (G-factor correction: $G = I_{Hv}/I_{Hh}$).

2.6. Atomic force microscopy

DMPC/DMPS (3:2, mol/mol) SLBs were prepared as described elsewhere [30]. Briefly, 50 μl of liposomes at 500 μM in 20 mM Tris, 150 mM NaCl, pH 7,40 and 10 mM $CaCl_2$ were incubated onto freshly cleaved mica at 50°C for 60 min. This method involved liposome fusion which did not allow controlling the lipid asymmetry. Non-adsorbed liposomes were eliminated by gently rinsing with the same buffer without Ca^{2+}. AFM intermittent contact mode images in liquid were obtained using a Nanoscaope IV Multimode AFM (Bruker AXS Corporation, Madison, WI) with MSNL silicon tips with a nominal spring constant of 30 pN · nm^{-1}. To minimize the applied force on the sample set point was continuously adjusted during imaging. Images were acquired at 0° scan angle at 1.5 Hz of scan rate. All images were processed using the Bruker software.

3. Results

3.1. Peptides characterization

The main objective of our study was focussed on the elucidation of the physicochemical properties of three peptides corresponding to the structural E2 capsid protein of GBV-C and their role in the inhibition of the FP-HIV. The rationale for choosing these sequences were differences found in previous experiments [22] that indicated the inhibitory activity of P45 on FP-HIV (formerly named Gp-41)-mediated cell-cell fusion assay in contrast to P58 and P59. First, we have compared their amino acid sequence and charge at the physiological pH (buffered saline solution, pH: 7.4) (Table 1). These sequences were selected from a series of overlapping peptides with a length of 18 amino acids included in the region 89–147 of the E2 capsid protein, [24]. Peptide neighbors differ in three amino acids. Thus, P58 and P59 share the fragment RFPFHRCGAGPKLTK and the three uncommon amino acids are DLE in P58 and GSV in P59. While P59 is able to inhibit the leakage of contents caused by FP-HIV in POPG liposomes, P58 doesn't. If we focus on the charge of the peptides at the pH under study, it is +6 for P58 and +4 for P59 and this could be the responsible of the differences observed in the test of inhibition of liposome leakage contents. On the other hand, P45 has a completely different sequence without any fragment in common having anionic character (−2). Charge is distributed along the peptide chain in P58 and P59 but not so in P45 that is concentrated in one side, conferring thus a hydrophobic character in the other side, making the peptide more susceptible to interact with the FP-HIV peptide that is positively charged. P45 shares with P59 its ability to inhibit FP-HIV liposomes contents leakage but at different peptide/FP-HIV molar ratio. In the case of P45/FP-HIV this ratio is 2:1 and for P59/FP-HIV, 5:1. Solubility was similar for the three peptides that were solubilized in acetonitrile/water (1:1, v/v) and therefore, differences in activity couldn't be attributed to hydrophobic/hydrophilic balance but to amino acid distribution along the peptide chain. A data to be considered is the ability to form hydrogen bonds with the medium that is around 33% for P58 and P59 and rises up to a 50% for P45.

3.2. Peptides surface activity and interaction with lipid monolayers.

Peptides showed concentration dependency on its surface activity. At low peptide concentrations the adsorption was gradual. The higher the peptide concentration in the subphase, the faster the incorporation process and the higher the surface pressure achieved. In all the cases, the pressure reached a constant value after 60 minutes indicating the equilibrium of the system. The shape of the surface activity curves approximates to a rectangular hyperbola and it was fitted to Eq. (2):

$$\pi = \frac{c\pi_{sat}}{K + c} \tag{2}$$

where *c* is the concentration, π_{sat} is the maximum pressure reached and *K* a constant that indicates the peptide concentration needed to reach half π_{sat}. A summary of the results is indicated in Table 1. Remarkably, P58 had the highest π_{sat}, almost three times higher than the measured for P45.

By applying the Gibbs equation, the surface excess concentration (Γ) of the peptides was calculated according to the equation:

$$\Gamma = \frac{1}{RT}\frac{\Delta\pi}{\Delta \ln c} \tag{3}$$

being *R* the gas constant, *T* the temperature (298 K), $\Delta\pi$ the surface pressure increase achieved after 60 minutes, and *c* the concentration of the peptide in the subphase. These results observed in Table 1, suggest equilibrium between the molecules of the peptides in solution and those at the air/water interface.

The surface excess concentration at saturation (Γ_{max}) calculated from the slope of the curve $\Delta\pi - \Delta \ln c$ can be found in Table 1. From these values we calculated the surface molecular area (*A*) according to the equation:

$$A = \frac{1}{\Gamma_{max} N} \tag{4}$$

where N is the Avogadro's constant.

Measurement of the surface activity of a molecule is a method used to estimate the molecular surface area, which in the case of flexible molecules can provide information about its conformational behavior [31]. The molecular areas obtained (Table 1) indicate the possibility of a α–helical conformation of the peptides with vertical orientation at the air–water interface [32]. Therefore, these similarities in molecular areas don't enable the discrimination of the peptides activity in basis to conformational changes.

A further step in the differentiation of peptides behavior was focused on the study of their interaction with lipid monolayers by

Table 2
Values of "*lift-off*" and extrapolated area or limiting indicate the area occupied by the molecule in the monolayer.

Peptide	*Area lift-off* (nm^2 molec^{-1})	*Limiting Area* (nm^2 molec^{-1})
P 59	0.57	1.75
P 58	0.40	1.75
P 45	0.33	1.50

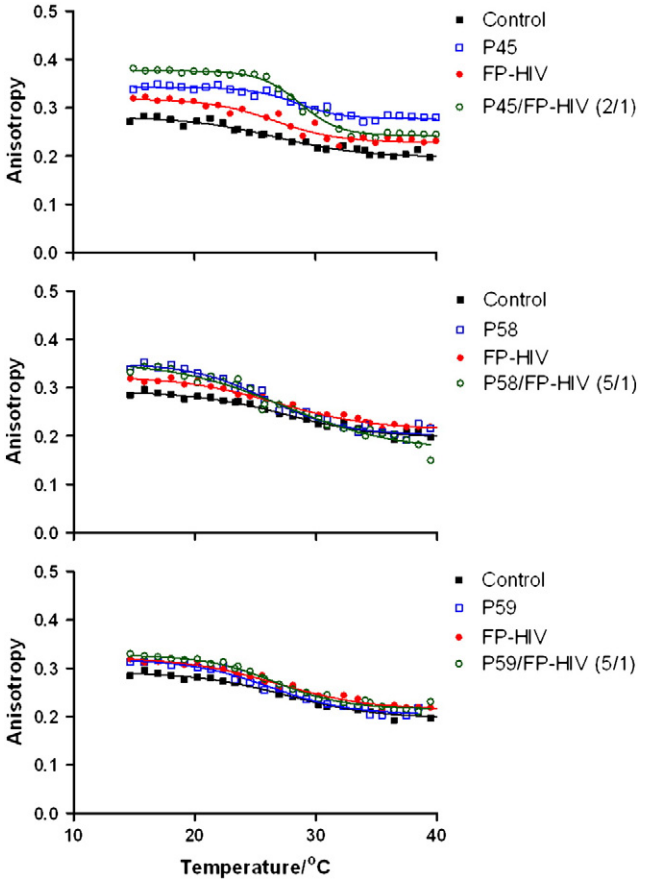

Fig. 1. Fluorescence anisotropy studies of the three peptides in DMPC/DMPS (3:2, mol/mol) LUVs labeled with the fluorescent probe TMA-DPH. The peptide/lipid molar ratio was 1:20 in buffered saline solution (Tris–HCl, pH: 7.4). Peptide and lipid concentration into the cuvette were 5 μM and 75 μM, respectively. In the case of GBV-C/FP-HIV, the peptide/peptide molar ratio was chosen according to the inhibition of liposome contents leakage obtained in [22].

means of penetration kinetics. The lipid composition was DMPC/DMPS (3:2, mol/mol) with anionic charge chosen to mimic cells infected with HIV [24]. Exclusion pressure that indicates the maximum penetration ability by the peptides into lipid monolayers was 45.6 mN m^{-1} and 40.7 mN m^{-1} for P58 and P59, respectively. These results were expected taking into consideration the data obtained in the previous section and the charge influence in peptide/lipid interaction as described for other similar peptides [19]. On another hand, the low insertion of P45 into phospholipid monolayers is likely due to the electrostatic repulsions since both peptide and lipid polar head are negatively charged.

3.3. Compression isotherms

π–A isotherms were measured to obtain basic information of the different peptides on the phase behavior under compression process. The amount of peptide extended on the air/buffered surface was in all the cases 1.6×10^{16} molecules. P45, P58 and P59 were able to form stable monolayers with a hysteresis cycle reproducible upon compression. Isotherms were characteristic of peptides with low molecular weight and show well differentiated regions from which we can obtain several characteristic parameters (Table 2). The lift-off area, defined as the mean molecular area when surface pressure has reached 1 mN m^{-1} [33] indicates that the peptides adopt an extended horizontal configuration in the monolayer [34]. Extrapolated area or limiting area indicates the area occupied by the molecule in the more condensed phase. In our experiments, these values increased also in the same order being closer to the theoretical value of 1.75 nm^2 $molec^{-1}$ found for a α-helix peptide oriented perpendicular to the interface [35].

3.4. Fluorescence anisotropy of membrane lipids

A step forward consisted in the analysis of the degree of peptide penetration into bilayers assessed by fluorescence anisotropy using two fluorescent probes that locate in different positions of the bilayer, DPH (hydrophobic) and TMA-DPH (partially hydrophilic). No interactions were observed in DMPC vesicles (zwitterionic) (data not shown) while different behavior was seen with liposomes composed of DMPC/DMPS (3:2, mol/mol) that hold negative charge. The peptides changed the properties of the hydrophilic part of the bilayer as stated by the results obtained with TMA-DPH (Fig. 1). As a general trend, incorporation of the peptides in the incubation media resulted in an increase in the anisotropy (*r*) all over the temperature range (15 to 40°C). This is a proof of an increase in bilayer rigidity as a consequence of the peptides. This change is more relevant for P45 and its mixture with FP-HIV, being the highest *r* values those obtained with P45/FP-HIV (2/1, mol/mol). P58, P59 and their mixtures with FP-HIV present similar values at a temperature below the T_m when the membrane is in a gel state. Above T_m the lines tend to superimpose that of the control but differences are still evident. In the case of DPH, anisotropy data is similar to the control at *T* below T_m of the lipid mixture. However, we can distinguish different effects above T_m depending on the peptide

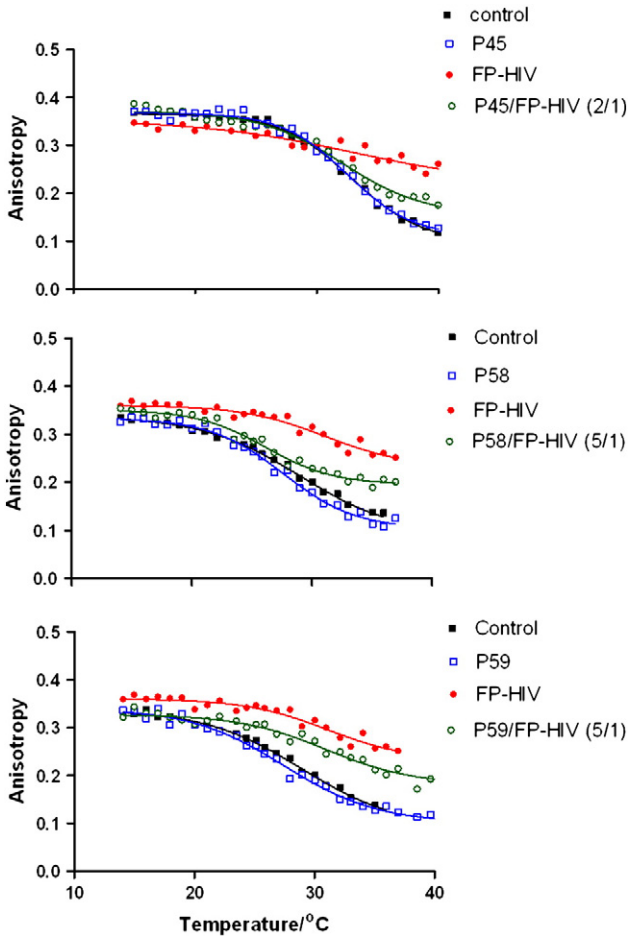

Fig. 2. Fluorescence anisotropy studies of the three peptides in DMPC/DMPS (3:2, mol/mol) LUVs labeled with the fluorescent probe DPH. The peptide/lipid molar ratio was 1:20 in buffered saline solution (Tris–HCl, pH: 7.4). Peptide and lipid concentration into the cuvette were 5 μM and 75 μM, respectively. In the case of GBV-C/FP-HIV, the peptide/peptide molar ratio was chosen according to the inhibition of liposome contents leakage obtained in [22].

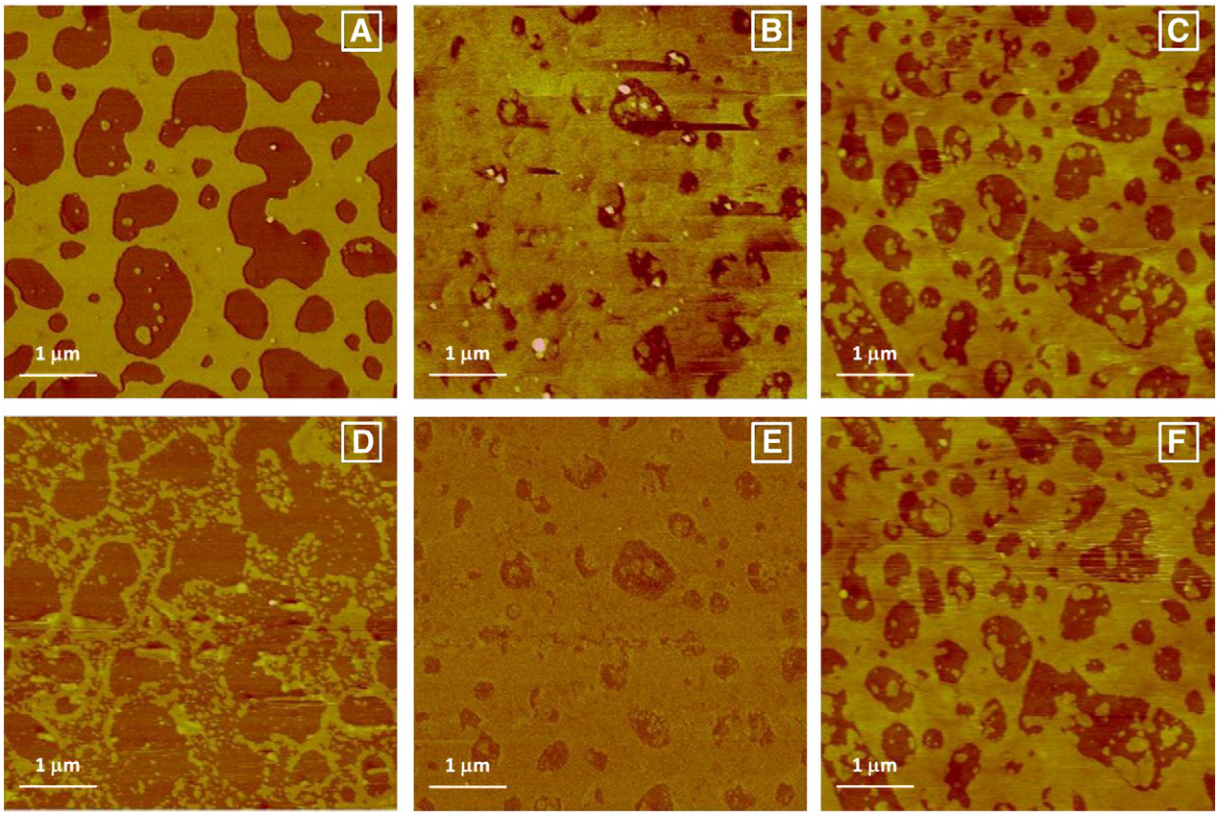

Fig. 3. AFM images of DMPC/DMPS (3:2, mol/mol) SLB before (A, B and C) and after incubation of: D) 5 μM FP-HIV, E) 10 μM P45 and F) 5 μM FP-HIV + 10 μM P45 for 30 min at room temperature. Z scale bar is 20 nm.

(Fig. 2). FP-HIV can penetrate into the liposomes increasing the rigidity of the lipid bilayer. This rigidifying effect is reduced by the presence of the peptides. Particularly interesting is the effect observed for P45 that almost abolishes FP-HIV penetration up to 35°C and, for that reason, this sequence was chosen for AFM studies.

3.5. Atomic force microscopy

AFM permits to visualize in real time the interaction of macromolecules with the surface of SLBs [30,36]. We have thus studied the interaction of the different peptides with SLBs of DMPC/DMPS (3:2, mol/mol) (Fig. 3). Fig. 3A, B and C represent the SLBs before the injection of the corresponding peptides. Height, roughness (*Ra*) and covering values can be found in Table 3. Fig. 3D shows the effect of the injection of FP-HIV on the SLB to a final concentration of 5 μM after 30 min of incubation. From the image it is clearly seen the destabilization of the SLB which results in a reduction of the thickness of the SLB from 5.3 to 4.1 nm. But more importantly, the addition of the FP-HIV promotes desorption of lipids composing the SLB as inferred from the decrease in the covering of the mica surface, from 55% to 30%. Fig. 3E shows the effect of the injection of P45 to a final concentration of 10 μM on the SLB after 30 min of incubation. In this case the SLB height is dramatically decreased, from 5.4 to 1.9 nm, together with an increasing of the surface covered by the SPB. In Fig. 3F it is shown the SLB after the injection of a mixture of FP-HIV and P45 in a molar ratio of 1:2 (5 μM FP-HIV and 10 μM of P45). In this case, after 30 min of incubation the SLB is mostly intact, both in height and in covering (see Table 3) suggesting a possible interaction of both peptides in solution before the interaction with the SLB.

To gain insight to this possible aggregation process we analyzed the molecular structure of the FP-HIV and P45 through its amino acid sequence [37]. The *de novo* approach permits to predict the structure of the FP-HIV and P45 peptides minimizing the energy. In Fig. 4A it is plotted the predicted structure at the minimum value of energy of FP-HIV from where it can be seen that FP-HIV presents a big hydrophobic region (pink ribbon). Therefore, FP-HIV may interact with the DMPC/DMPS (3:2, mol/mol) SLB through its hydrophobic region eroding the SLB surface to form peptide–lipid mixed micelles. In Fig. 4B it is depicted the predicted structure at the minimum value of energy of P45 peptide. From this image it is clearly seen that P45 is formed mainly by two β-sheet structures (yellow flat arrows). In this case the interaction of P45 with the SLB composed of DMPC:DMPS is not so clear as before: i) P45 can be adsorbed by its β-sheet structures flat to the SPB surface; ii) P45 can be absorbed inside of the SPB exposing the charged amino acids towards the liquid media. Regardless of how the peptide interacts with the SLB it is not able to form holes that could disintegrate the SLB, under our experimental conditions. Moreover, it seems to facilitate the spreading of the SLB decreasing the line tension existing between the lipids forming the SLB. In Fig. 4C it is depicted a possible interaction between FP-HIV and P45, taking into account that: I) the hydrophobic regions of both peptides could protect each other from their exposure to the water environment, fact that could explain why the peptides incubated together nearly do not interact with the SLBs, and ii) the molar ratio of 1 molecule of FP-

Table 3
Height, roughness (*Ra*) and covering percentage values of the SLBs before and after 30 min of peptide incubation.

		SLB		
		FP-HIV	P45	FP-HIV + p45
0 min	*h* (nm)	5.3 ± 0.3	5.4 ± 0.4	5.5 ± 0.3
	Ra (nm)	0.018	0.3	0.5
	Covering (%)	55	78	63
30 min	*h* (nm)	4.1 ± 0.4	1.9 ± 0.4	4.9 ± 0.5
	Ra (nm)	–	0.3	0.6
	Covering (%)	30	86	60

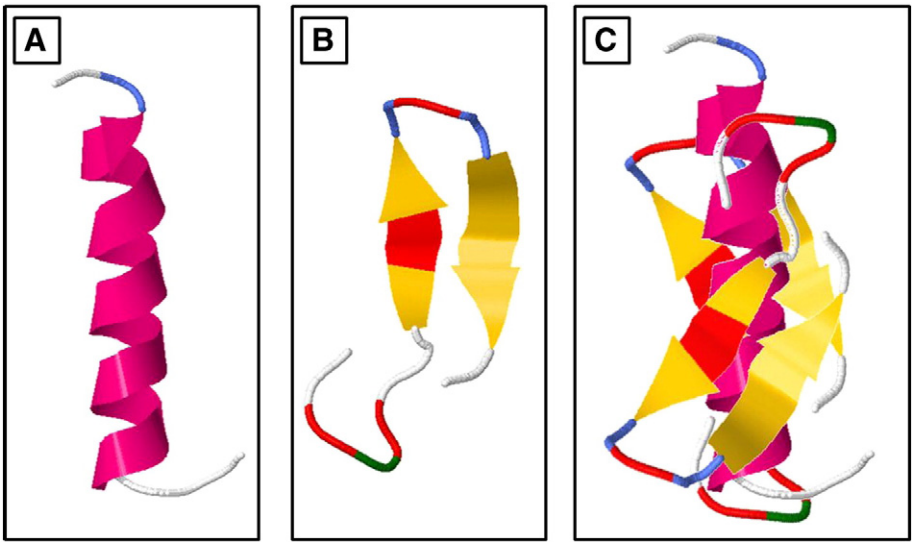

Fig. 4. Predicted molecular structures at the minimum value of energy for FP-HIV A), P45 B) and a possible molecular organization, in solution, of the FP-HIV-P45 mixture C). Color meanings, pink: α-helix; yellow: β-sheet; red: anionic amino acid; green: cationic amino acid; blue: β-turn and white: unspecific.

HIV with two molecules of P45 seems to be enough to inhibit their own actions on the SLB.

4. Conclusions

The surface studies indicate that the three sequences have different activity and ability to penetrate into lipid monolayers (Tables 1 and 2) as a consequence of their amino acid distribution. Even though the peptide charge isn't a determinant data to define their surface activity, it is of great relevance in their penetration into DMPC/DMPS (3:2, mol/mol) monolayers. P45 lacks of interaction with lipid monolayers of this composition because both, peptide and lipids, are negatively charged and repulsion forces are dominant. The contrary is observed with P58 and P59 that are positively charged and can insert into the monolayer up to exclusion pressures higher than 32 mN m^{-1} that is the minimum value that predicts the penetration into the biological membranes. On another hand, when considering the effect of these peptides in lipid bilayers, the results from fluorescence anisotropy show that the three peptides can modify the membrane behavior of the outer part of the bilayer increasing its rigidity. However, the behavior is similar for all the peptides and no changes in FP-HIV are observed in presence of any of the GBV-C sequences. On another hand, studies of the interaction of the peptides with the inner core of the membrane labeled with DPH showed that the three peptides were able to decrease the rigidifying effect of FP-HIV in the bilayer. This was more relevant for P45 than for P58 or P59. For that reason, P45 has chosen for further experiments to elucidate the changes involved in bilayer morphology in presence and absence of FP-HIV.

From AFM images can be inferred different modes of action of FP-HIV and P45. On one hand, FP-HIV interacts with the SLB eroding and solubilizing the surfaces of the lipid bilayer while the edges of the SLB were unaltered. Due to lipid was not deposited on the exposed mica it is reasonable to suppose that solubilized lipids were set aside from the scanned region. On the other hand, P45 does not destroy the SLB. From the image it seems that P45 absorbs into the SLB decreasing the lateral surface pressure inside of the SLB, fact that promotes the spreading of the lipids in the SLB on the exposed mica surface. As expected by results previously discussed in this paper, when FP-HIV and P45 are incubated together at a molar ratio of 1:2 neither the solubilization nor the spreading effects of the SLB were observed. When both peptides are mixed before the injection on the SLB, they seem to form aggregates blocking to each other their active regions against the SLB. Therefore, it is reasonable to conceive an aggregate in solution where the β-sheets from P45 could cover the α-helix structure of FP-HIV. Therefore this new conformation could prevent the anchorage of FP-HIV to the SLB surface impeding the formation of holes that would destroy the SLB.

Acknowledgements

This work was supported by Grants CTQ2012-37589-C02-01/02 from the Ministerio de Economía y Competitividad and 2009 SGR 560 from the Generalitat de Catalunya.

References

[1] A. Loffet, Peptides as Drugs: Is There a Market? J. Pept. Sci. 8 (2002) 1–7.
[2] A. Vandenbark, E. Morgan, R. Bartholomew, D. Bourdette, R. Whitham, D. Carlo, D. Gold, G. Hashim, H. Offner, TCR peptide therapy in human autoimmune diseases, Neurochem. Res. 26 (2001) 713–730.
[3] K. Kessenbrock, R. Raijmakers, M.J. Fritzler, M. Mahler, Synthetic peptides: the future of patient management in systemic rheumatic diseases? Curr. Med. Chem. 14 (2007) 2831–2838.
[4] E. Koivunen, W. Arap, H. Valtanen, A. Rainisalo, O.P. Medina, P. Heikkila, C. Kantor, C.G. Gahmberg, T. Salo, Y.T. Konttinen, T. Sorsa, E. Ruoslahti, R. Pasqualini, Tumor targeting with a selective gelatinase inhibidor, Nat. Biotechnol. 17 (1999) 768–774.
[5] H. Yin, J.P. Saludes, L.A. Morton, Compositions, methods and uses for peptides in diagnosis, progression and treatment of cancers, PCT, Int. Appl.2012. (US2012/053225).
[6] C.J. Wikstrand, L.P. Hale, S.K. Batra, M.L. Hill, P.A. Humphrey, S.N. Kurpad, R.E. McLendon, D. Moscatello, C.N. Pegram, C.J. Reist, Monoclonal antibodies against EGFRvIII are tumor specific and react with breast and lung carcinomas and malignant gliomas, Cancer Res. 55 (1995) 3140–3148.
[7] T. Zhewei, F. Mingqian, G. Wei, Y. Phung, W. Chen, A. Chaudhary, B.S. Croix, M. Qian, D.S. Dimitrov, M. Ho, A human single-domain antibody elicits potent anti-tumor activity by targeting an epitope in mesothelin close to the cancer cell surface, Mol. Cancer Ther. (2013), http://dx.doi.org/10.1158/1535-7163.
[8] V.R. De Soultrait, C. Desjobert, L. Tarrago-Litvak, Peptides as new 19structura of HIV-1 reverse transcriptase and integrase, Curr. Med. Chem. 10 (2003) 1765–1778.
[9] O. Taboga, C. Tami, E. Carrillo, J.I. Nunez, A. Rodriguez, J.C. Saiz, E. Blanco, M.L. Valero, X. Roig, J.A. Camarero, D. Andreu, M.G. Mateu, E. Giralt, E. Domingo, F. Sobrino, E.L. Palma, A large-scale evaluation of peptide vaccines against foot-and-mouth disease: lack of solid protection in cattle and isolation of escape mutants, J. Virol. 71 (1997) 2606–2614.
[10] S.A. Perez, E. von Hofe, N.L. Kallinteris, A.D. Gritzapis, G.E. Peoples, M. Papamichail, C.N. Baxevanis, A new era in anticancer peptide vaccines, Cancer 116 (2010) 2071–2080.
[11] R.H. Meloen, W.C. Puijk, J.P.M. Langeveld, J.P.M. Langedijk, P. Timmerman, Design of synthetic peptides for diagnostics, Curr. Protein Pept. Sci. 4 (2003) 253–260.
[12] L.V. Ly, M. Sluijter, S.H. Van der Burg, M.J. Jager, T. Van Hall, Effective cooperation of monoclonal antibody and peptide vaccine for the treatment of mouse melanoma, J. Immunol. 190 (2013) 489–496.
[13] S. Fournel, S. Muller, Synthetic peptides in the diagnosis of systemic autoimmune disease, Curr. Protein Pept. Sci. 4 (2003) 261–276.
[14] M.C. Alcaro, E. Peroni, P. Rovero, A.M. Papini, Synthetic peptides in the diagnosis of HIV infection, Curr. Protein Pept. Sci. 4 (2003) 285–290.
[15] M.J. Gomara, I. Haro, Synthetic peptides for the immunodiagnosis of human diseases, Curr. Med. Chem. 14 (2007) 531–546.

[16] D. Brown, L. Powell, A. Morris, S. Rassam, S. Sherlock, N. McIntyre, A.J. Zuckerman, G.M. Dusheiko, Improved diagnosis of chronic hepatitis C virus infection by detection of antibody to multiple epitopes: confirmation by antibody to synthetic oligopeptides, J. Med. Virol. 38 (1992) 167–171.
[17] T.M. Wisniewski, F. Goni, Immunotherapeutic modulation of amyloidogenic disease using non-fibrillogenic, non-amyloidogenic polymerized proteins and peptides, PCT, Int. Appl. (2013) (WO 2013012811 A2 20130124).
[18] M.L. Perez, M.J. Gomara, G. Ercilla, R. Sanmarti, I. Haro, Antibodies to citrullinated human fibrinogen synthetic peptides in diagnosing rheumatoid arthritis, J. Med. Chem. 50 (2007) 3573–3584.
[19] M. Alay, I. Haro, V. Girona, J. Prat, M.A. Busquets, Interaction of two overlapped synthetic peptides from GB virus C with charged mono and bilayers, Colloids Surf. B: Biointerfaces 105 (2013) 7–13.
[20] N. Bhattarai, J.T. Stapleton, GB virus C: the good boy virus? Trends Microbiol. 20 (2012) 124–130.
[21] W. Zhang, K. Chaloner, H.L. Tillmann, C.F. Williams, J.T. Stapleton, Effect of early and late GB virus C viraemia on survival of HIV-infected individuals: a meta-analysis HIV, Medicine 7 (2006) 173–180.
[22] E. Herrera, S. Tenckhoff, M.J. Gómara, R. Galatola, M.J. Bleda, C. Gil, G. Ercilla, J.M. Gatell, H.L. Tillmann, I. Haro, Effect of synthetic peptides belonging to E2 envelope proetin of GB virus C on human immunodeficiency virus type 1 infection, J. Med. Chem. 53 (2010) 6054–6063.
[23] P. Dynarowicz-Latka, A. Dhanabalan, O.N. Jr, Oliveira, Modern physiochemical research on Langmuir monolayers, Adv. Colloid Interface Sci. 91 (2001) 221–293.
[24] N. Lev, Y. Fridmann-Sirkis, L. Blank, A. Bitler, F.R. Epand, R.M. Epand, S. Shai, Conformational Stability and Membrane Interaction of the Full-Length Ectodomain of HIV-1 gp41: Implication for Mode of Action, Biochemistry 48 (2009) 3166–3175.
[25] I. Haro, M.J. Gomara, R. Galatola, O. Domenech, J. Prat, V. Girona, M.A. Busquets, Study of the inhibition capacity of a 18-mer peptide domain of GBV-C virus on gp41-FP HIV-1 activity, Biochim. Biophys. Acta Biomembr. 1808 (2011) 1567–1573.
[26] D.J. Muller, AFM: A nanotool in membrane biology, Biochem. 47 (2008) 7986–7998.
[27] M. Rafalski, J.D. Lear, W.F. De Grado, Phospholipid interactions of synthetic peptides 21structural the N-terminus of HIV gp41, Biochem. 29 (1990) 7917–7922.
[28] C.W.F. McClare, An accurate and convenient 21struct phosphorus assay, Anal. Biochem. 39 (1971) 527–530.
[29] L.M. Souza-Fagundes, A.O. Frank, M.D. Feldkamp, D.C. Dorset, W.J. Chazin, O.W. Rossanese, E.T. Olejniczak, S.W. Fesik, A high-throughput fluorescence polarization anisotropy assay for the 70 N domain of replication protein A, Anal. Biochem. 421 (2012) 742–749.
[30] Ò. Domènech, Y. Dufrêne, F. van Bambeke, P.M. Tulkens, M.P. Mingeot-Leclercq, Interactions of oritavancin, a new semi-synthetic lipoglycopeptide, with lipids extracted from *Staphylococcus aureus*, Biochim. Biophys. Acta Biomembr. 1798 (2010) 1876–1885.
[31] J. Cantó, J.A. Pérez, N.B. Centeno, I. Haro, J.J. Pérez, Conformational study of the preferred conformations of the peptide sequence VP3(110–121) of HAV by circular dichroism and molecular mechanics, Lett. Pept. Sci. 4 (1997) 413–419.
[32] R. Maget-Dana, D. Lelièvre, A. Brack, Surface active properties of amphiphilic sequential isopeptides: Comparison between α-helical and β-sheet conformations, Biopolym. 49 (1999) 415–423.
[33] N. Vila Romeu, J. Miñones Trillo, O. Conde, M. Casas, E. Iribarnegaray, Mixed calcitonin — poly[(d, l-lactic acid)-co-(glycolic acid)] monolayers, Langmuir 13 (1997) 71–75.
[34] S. Steinkopf, A.K. Schelderup, H.I. Gjerde, J. Feiffer, S.V. Thoresen, A.U. Gjerde, H. Holmsen, The psychotropic drug olanzapine (Zyprexa®) increases the area of acid glycerophospholipid monolayers, Biophys. Chem. 134 (2008) 39–46.
[35] E.E. Ambrogio, F. Separovic, J. Bowie, G.D. Fidelio, Surface behaviour and peptide-lipid interactions of the antibiotic peptides, maculatin and citropin, Biophys. Acta 1664 (2004) 31–37.
[36] O. Domènech, L. Redondo, M.T. Montero, J. Hernández-Borrell, Specific adsorption of cytochrome c on cardiolipin-glycerophospholipid monolayers and bilayers, Langmuir 23 (10) (2007) 5651–5656.
[37] C. Alland, F. Moreews, D. Boens, M. Carpentier, S. Chiusa, M. Lonquety, N. Renault, Y. Wong, H. Cantalloube, J. Chomilier, J. Hochez, J. Pothier, B.O. Villoutreix, J.F. Zagury, P. Tufféry, A web resource for 22structural bioinformàtics, Nucleic Acids Res. 1 (2005) 33 ((Web Server issue):W44-9).